Supporting Information

In situ topotactic synthesis of porous network $Zn_2Ti_3O_8$ platelike nanoarchitecture and its long-term cycle performance for LIBs anode

Xingang Kong[a]*, Xing Wang[a], Dingying Ma[a], Jianfeng Huang[a], Jiayin Li[a], Ting Zhao[a], Lixiong Yin[a], Qi Feng[ab]*

[a] School of Materials Science and Engineering, Shaanxi University of Science and Technology, Weiyang, Xi'an, Shaanxi 710021, PR China

[b] Department of Advanced Materials Science, Faculty of Engineering, Kagawa University, 2217-20 Hayashi-cho, Takamatsu-shi, 761-0396 Japan

*Author to whom correspondence should be addressed. E-mail: yezhu_1983@163.com, feng@eng.kagawa-u.ac.jp

Tab. S1 XRF analysis results of Zn/Ti molar ratio of sample.

Sample	**Zn/Ti molar ratio**
Zn-HTO	0.51:1.73
Product after heat-treatment of Zn-HTO	0.51:1.73
Zn-H_2O_2-HTO	1.07:1.73
Product after heat-treatment Zn-H_2O_2-HTO	1.07:1.73

Tab. S2 Zeta potential of HTO before and after the H_2O_2 pretreatment.

Sample	**Zeta potential (mV)**
HTO	-581 mV (ethanol system)
	-26.3 mV (water system)
H_2O_2-HTO	$-3.31X10^4$ mV (ethanol system)
	-41.9 (water system)

Sample Name:	3 1		
SOP Name:	mansettings.nano		
File Name:	Example Results.dts	**Dispersant Name:**	Water
Record Number:	1251	**Dispersant RI:**	1.330
Date and Time:	2018年1月24日 19:38:34	**Viscosity (cP):**	0.8872
		Dispersant Dielectric Constant:	78.5

Temperature (°C):	25.0	**Zeta Runs:**	12
Count Rate (kcps):	237.1	**Measurement Position (mm):**	2.00
Cell Description:	Green disposable zeta cell	**Attenuator:**	8

			Mean (mV)	**Area (%)**	**St Dev (mV)**
Zeta Potential (mV):	-26.3	**Peak 1:**	-26.3	100.0	9.55
Zeta Deviation (mV):	9.55	**Peak 2:**	0.00	0.0	0.00
Conductivity (mS/cm):	0.0229	**Peak 3:**	0.00	0.0	0.00

Result quality : **See result quality report**

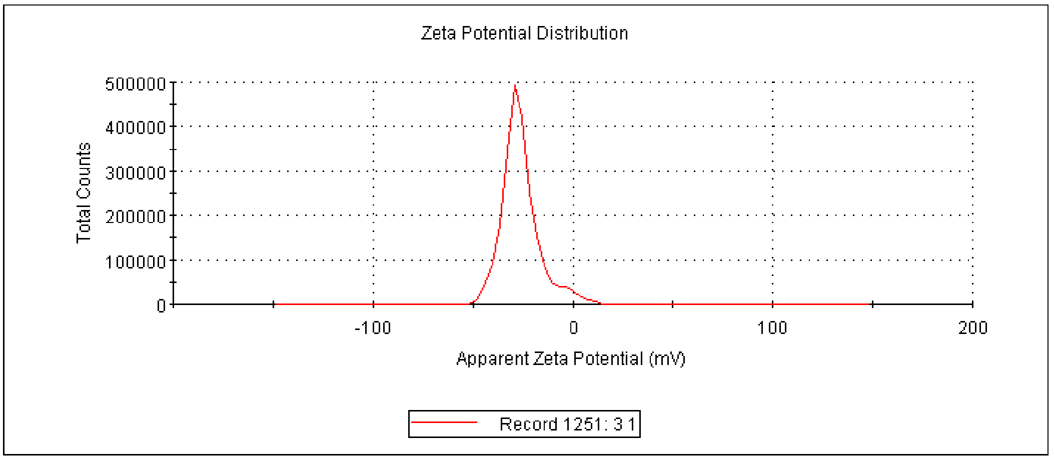

Raw data of Zeta potentials (HTO in water system)

Sample Name:	4 1		
SOP Name:	mansettings.nano		
File Name:	Example Results.dts	**Dispersant Name:**	乙醇
Record Number:	1253	**Dispersant RI:**	1.480
Date and Time:	2018年1月24日 19:42:41	**Viscosity (cP):**	3.6720
		Dispersant Dielectric Constant:	0.100

Temperature (°C):	25.0	**Zeta Runs:**	100
Count Rate (kcps):	317.9	**Measurement Position (mm):**	2.00
Cell Description:	Green disposable zeta cell	**Attenuator:**	7

			Mean (mV)	**Area (%)**	**St Dev (mV)**
Zeta Potential (mV):	-581	**Peak 1:**	0.102	100.0	150
Zeta Deviation (mV):	1.57e4	**Peak 2:**	0.00	0.0	0.00
Conductivity (mS/cm):	0.00209	**Peak 3:**	0.00	0.0	0.00

Result quality : **See result quality report**

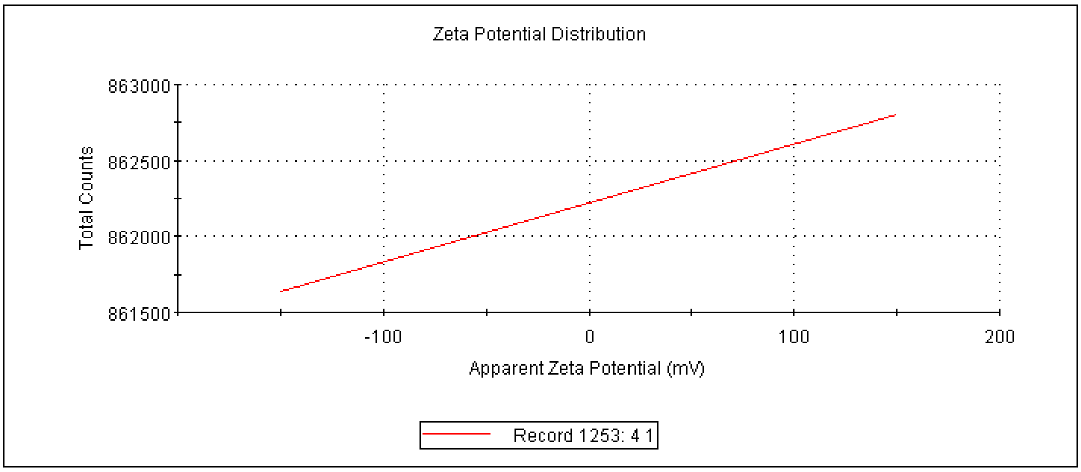

Raw data of Zeta potentials (HTO in ethanol system)

Sample Name:	1 1		
SOP Name:	mansettings.nano		
File Name:	Example Results.dts	**Dispersant Name:**	Water
Record Number:	1248	**Dispersant RI:**	1.330
Date and Time:	2018年1月24日 19:29:57	**Viscosity (cP):**	0.8872
		Dispersant Dielectric Constant:	78.5

Temperature (°C):	25.0	**Zeta Runs:**	12
Count Rate (kcps):	205.4	**Measurement Position (mm):**	2.00
Cell Description:	Green disposable zeta cell	**Attenuator:**	8

			Mean (mV)	**Area (%)**	**St Dev (mV)**
Zeta Potential (mV):	-41.9	**Peak 1:**	-39.2	64.4	5.54
Zeta Deviation (mV):	10.4	**Peak 2:**	-53.0	30.6	4.64
Conductivity (mS/cm):	0.0135	**Peak 3:**	-20.6	4.1	3.72

Result quality : See result quality report

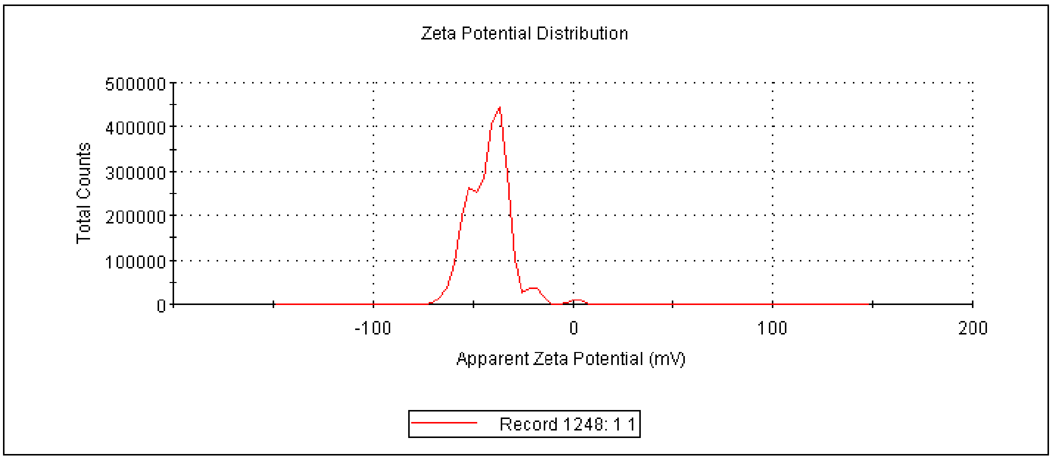

Raw data of Zeta potentials (H_2O_2-HTO in water system)

Sample Name:	2 1		
SOP Name:	mansettings.nano		
File Name:	Example Results.dts	**Dispersant Name:**	乙醇
Record Number:	1250	**Dispersant RI:**	1.480
Date and Time:	2018年1月24日 19:33:57	**Viscosity (cP):**	3.6720
		Dispersant Dielectric Constant:	0.100

Temperature (°C):	25.0	**Zeta Runs:**	32
Count Rate (kcps):	76.5	**Measurement Position (mm):**	2.00
Cell Description:	Green disposable zeta cell	**Attenuator:**	6

			Mean (mV)	**Area (%)**	**St Dev (mV)**
Zeta Potential (mV):	-3.31e4	**Peak 1:**	-3.17	100.0	150
Zeta Deviation (mV):	1.47e4	**Peak 2:**	0.00	0.0	0.00
Conductivity (mS/cm):	0.00163	**Peak 3:**	0.00	0.0	0.00

Result quality : Good

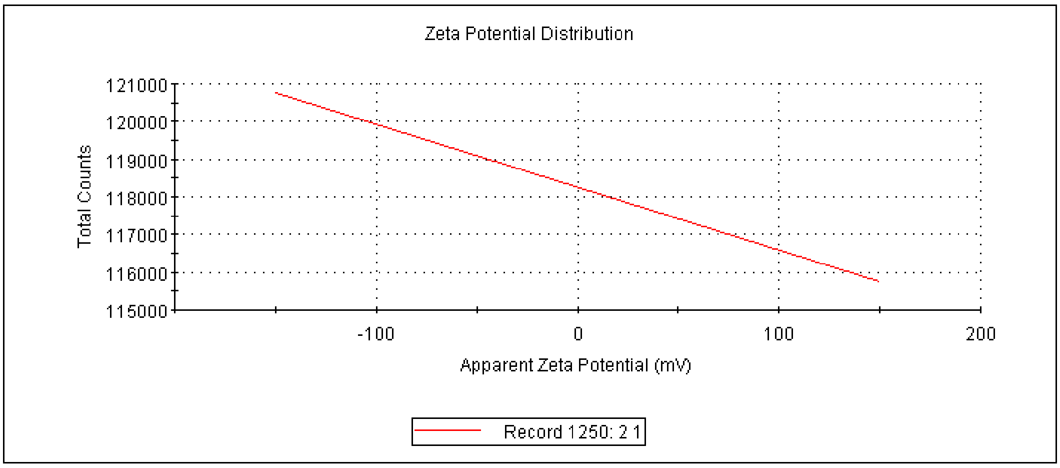

Raw data of Zeta potentials (H_2O_2-HTO in ethanol system)

Tab. S3 All of literature reports about the discharge capacity of $Zn_2Ti_3O_8$.

Material	Synthesis method	microstructure	Specific capacity (mA h g^{-1})	Current density	Active material: Acetylene black: PVDF	References
$Zn_2Ti_3O_8$	H_2O_2 assisted ion-exchange and heat treatment	Nanoarchitecture with porous network structure	423 (100 cycles) 408 (1000 cycles)	100mAh g^{-1} 1Ah g^{-1}	7:2:1	This work
$Zn_2Ti_3O_8$	Ion-exchange and heat treatment	Nanowires	400 (50 cycles)	100mAh g^{-1}	5:4:1	Hong Z et al[1]
$Zn_2Ti_3O_8$	molten-salt method	Nanoparticles	246	100mAh g^{-1}	8:1:1	Wang J et

			(450 cycles)			al[2]
$Zn_2Ti_3O_8$	Ion-exchange and template method	Hollow spheres	186.2 (300 cycles)	100mAh g^{-1}	7:2:1	Liao W et al[3]

1. Z. Hong, M. Wei, Q. Deng, X. Ding, L. Jiang and K. Wei, Chem. Commun., 2010, **46**, 740-742.

2. W. Liao, J. Tian, Z. Shan, R. Na, L. Cui and H. Lin, *Electrochim. Acta*, 2016, **216**, 94-101.

3. J. Wang, J. Zhang, Y. Zhang, J. Guo and J. Zhang, *J. Alloy. Compd.*, 2016, **688**, 392-398.

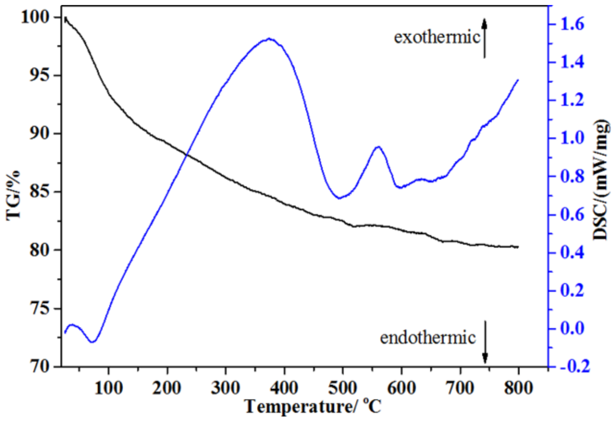

Fig. S1 TG-DSC curves of Zn-H_2O_2-HTO sample.

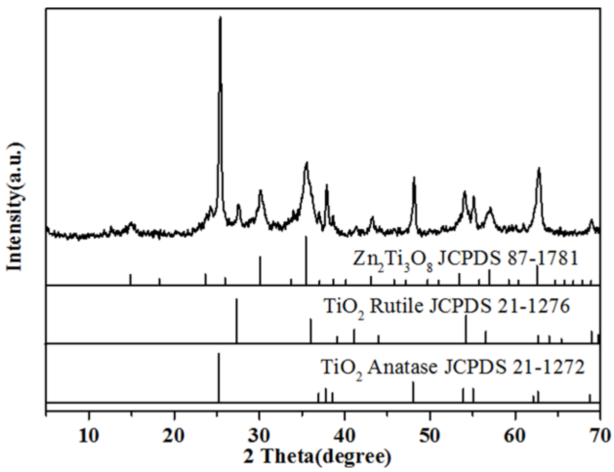

Fig. S2 XRD pattern of product after the heat-treatment of Zn-HTO at 600 °C

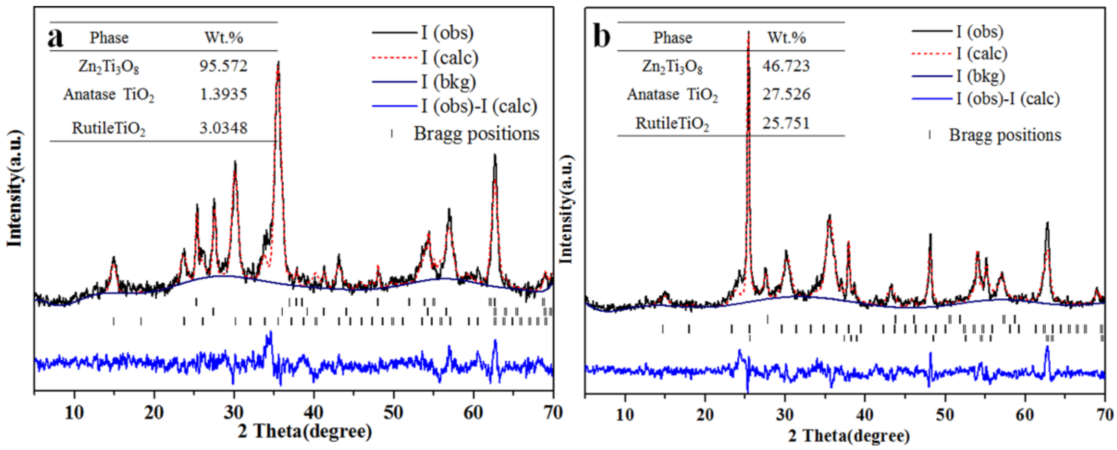

Fig. S3 Experimental XRD patterns (solid lines) and calculated patterns (dotted red line) of products after the heat-treatment of Zn-H_2O_2-HTO (a) and Zn-HTO (b) at 600 °C. The vertical marks indicate the position of Bragg peaks, and the bottom line shows the differences between the observed and calculated intensities. The calculated compositions are also shown.

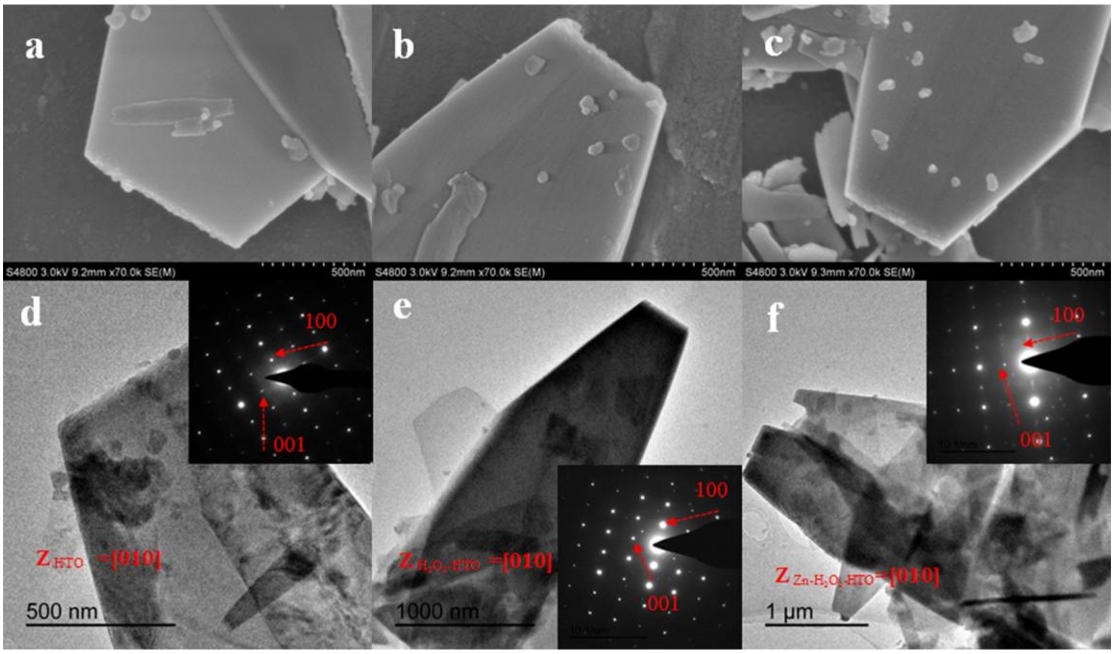

Fig. S4 FE-SEM images, TEM images and SAED pattern of HTO (a,d), H_2O_2-HTO (b,e) and Zn-H_2O_2-HTO (c,f).

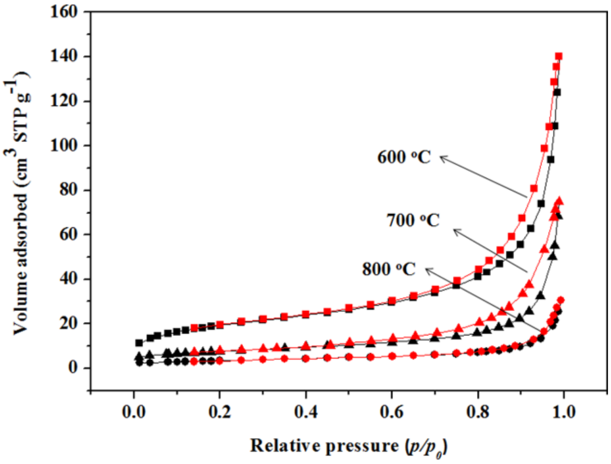

Fig. S5 Nitrogen adsorption/desorption isotherms of $Zn_2Ti_3O_8$ obtained at 600, 700 and 800 °C

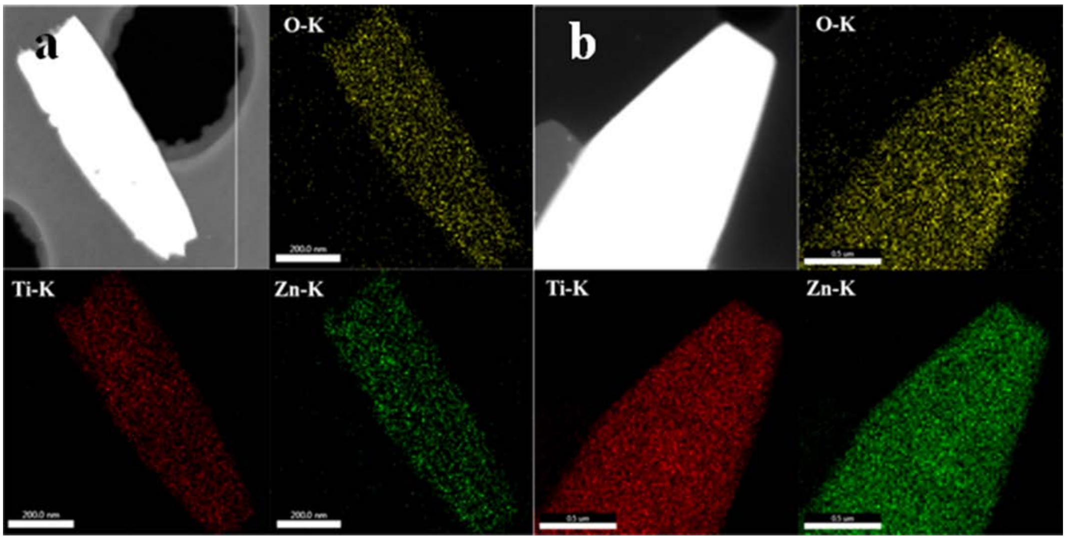

Fig. S6 EDS elemental mapping images of products after the heat-treatment of Zn-H_2O_2-HTO (a) and Zn-HTO (b) at 600 °C.

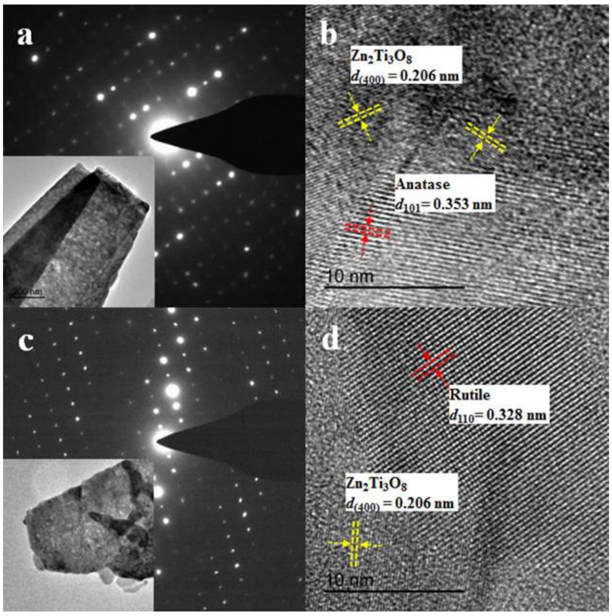

Fig. S7 SAED patterns and HRTEM images of products after the heat-treatment of Zn-H_2O_2-HTO at 700 (a,b) and 800 °C (c,d).

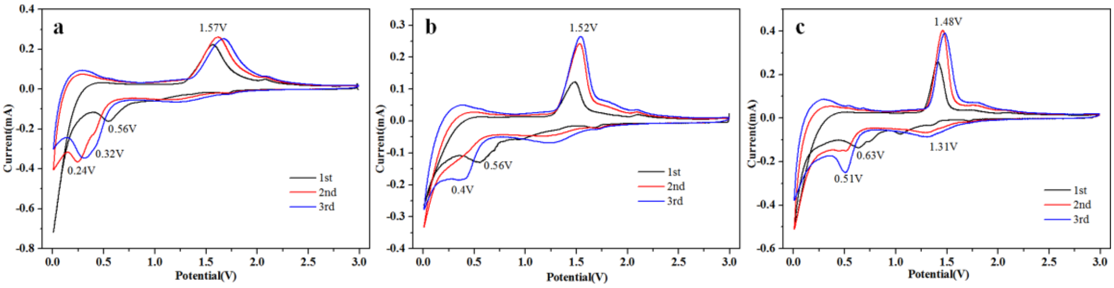

Fig. S8 The cyclic voltammograms (CVs) of products after the heat-treatment of Zn-H_2O_2-HTO at 600 (a), 700 (b) and 800 °C (c).

Fig. S8 present the cyclic voltammetry of $Zn_2Ti_3O_8$ electrodes obtained at 600, 700 and 800 °C, which was carried out at room temperature in the range of 0.01–3.0 V at a scan rate of 0.1mV s^{-1}. It is found that The $Zn_2Ti_3O_8$ electrodes obtained at different temperature show similar CV curves. A cathodic peak appears at 0.56V in the first cycle is attributed to the formation of solid electrolyte interface film at first cycle (this peak is not observed during following cycles). A pair of redox peaks located at about 1.54/1.33 V is related to Ti^{4+}/Ti^{3+} redox couple, implying that the lithium-ion intercalation/deintercalation into/out of the electrodes is reversible. And a cathodic peak found at 0.3 V during the second and third cycles might result from multiple restoration of Ti^{4+}[3-5].

4. W. J. H. Borghols, M. Wagemaker, U. Lafont, E. M. Kelder and F. M. Mulder, *J. Am. Chem. Soc.*, **131**,17786-17792.

5. H. Ge, N. Li, D. Li, C. Dai and D. Wang, *Electrochem. Commun.*, 2008, **10**, 719-722.

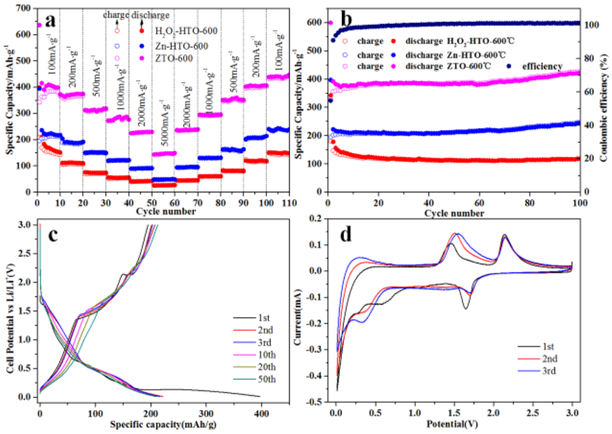

Fig. S9 (a)rate capability from 100 to 5000 mA g^{-1}, (b)cycling performance of $Zn_2Ti_3O_8/TiO_2$ at 100 mA g^{-1}, (c)voltage profiles under 100 mA g^{-1}; (d) cyclic voltammograms.

H_2O_2-HTO-600: TiO_2 obtained by heat treating H_2O_2-HTO at 600 °C

Zn-HTO-600: $Zn_2Ti_3O_8/TiO_2$ obtained by heat treating Zn^{2+} ion-exchanged HTO sample at 600 °C

ZTO-600: $Zn_2Ti_3O_8$ nanoarchitecture obtained at 600 °C

Fig. S9a shows the rate performance of H_2O_2-HTO-600, Zn-HTO-600 and ZTO-600. The H_2O_2-HTO-600 electrode represents the worst performance among three electrodes. At the current density of 100 mA g^{-1}, ZTO-600 displays the capacity of 406 mAh g^{-1} while Zn-HTO-600 shows the capacity of 221 mAh g^{-1}. The capacities of ZTO-600 and Zn-HTO-600 are 368 and 189 mAh g^{-1} at a current density of 100 mA g^{-1}. When the current density increases to 1A g^{-1}, they show the capacity of 273 and 121 mAh g^{-1}. While the current density is returned to 100m A g^{-1}, ZTO-600 exhibits a higher capacity of 439 mAh g^{-1} compared with that of Zn-HTO-600 (236 mAh g^{-1}). It is found that ZTO-600 electrode shows more excellent rate performance that that of Zn-HTO-600 electrode, which is due to the larger specific surface area and its porous network structure, meaning the more effective contact areas of active materials, conductive additives, and shorter lithium ion diffusion paths.

The cycle performances of Zn-HTO-600 and ZTO-600 are shown in Fig. S9b. Zn-HTO-600 displays a lower capacity of 100 mAh g^{-1} at the first few cycles and maintains no change after 100 cycles. ZTO-600 shows a discharge capacity of 599 mAh g^{-1} while Zn-HTO-600 exhibits a discharge capacity of 396 mAh g^{-1}at first cycles. After few cycles, the capacities of ZTO-600 and $Zn_2Ti_3O_8/TiO_2$ at 600 °C are 381 and 216 mAh g^{-1} respectively. The capacities of them nearly remain unchanged after 100 cycles. It is believed that ZTO-600 has a better cycle performance and good cycle stability.

Fig. S9c presents the first charge/discharge profiles of Zn-HTO-600 at different cycles under the current density of 100 mA g^{-1} tested for 100 cycles. The initial discharge and charge capacities are 396 and 195 mAh g^{-1}, the discharge capacity decreases to 220 mAh g^{-1} at the second cycle, and keeps unchanged in the following cycles with the coulombic efficiencies of almost 100%. Although Zn-HTO-600 has good cycle stability, the capacity is still low.

Cyclic voltammogram (CV) of Zn-HTO-600 is displayed in Fig S9d. A cathodic peak appears at 0.6V in the first cycle is attributed to the formation of solid electrolyte interface film at first cycle. A pair of redox peaks located at about 2.1/1.6 V is related to Ti^{4+}/Ti^{3+} redox couple of TiO_2 in Zn-HTO-600. The peaks at 2.1 and 1.6 V belonging to TiO_2 are not observed in $Zn_2Ti_3O_8$ at 600 °C which may be due to the lower content and weak crystallinity of TiO_2 in the sample. And a pair of redox peaks at about 1.54/1.33 V corresponds to Ti^{4+}/Ti^{3+} redox couple of $Zn_2Ti_3O_8$ in Zn-HTO-600. The cathodic peak found at 0.3 V during the second and third cycles might result from multiple restoration of Ti^{4+}.

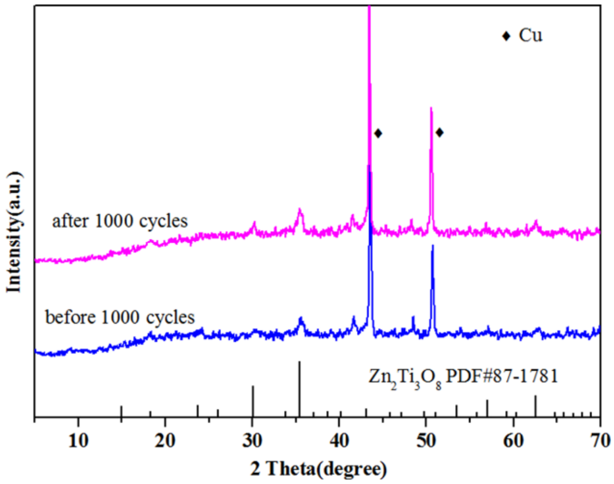

Fig. S10 The *ex-situ* XRD patterns of the electrode materials before and after tested for 1000 cycles.